

# Corrosive Crack and its 3D Defects Identification of Reinforced Concrete Subjected to Coupled Effect of Chloride Ions and Sulfate Ions

Jin Zuquan<sup>1,\*</sup>, Gao Song<sup>1</sup>, Zhao Xia<sup>2,\*</sup>, Yang Li<sup>1</sup>

<sup>1</sup> College of Civil Engineering, Qingdao Technological University, Qingdao, China

<sup>2</sup> Institute of Oceanology, Chinese Academy of Science, Qingdao, China

\*E-mail: [jinzuan@126.com](mailto:jinzuan@126.com), [zhxiakk@163.com](mailto:zhxiakk@163.com)

Received: 3 September 2014 / Accepted: 12 November 2014 / Published: 2 December 2014

---

Corrosive crack influenced by coupled effects of chloride and sulfate often occurs in marine and saline ground environment, which has been a very serious threat to the durability of reinforced concrete structures. In this paper, accelerated potentiostatic corrosion test was used to investigate the corrosive crack of reinforced concrete mixing with different content of chloride ions and sulfate ions. The evolution of electric current and surface cracks width of reinforced concrete was tested. The results indicated that the higher concentration of chloride ions in mixing water had, the larger electric current intensity between the deformed steel bar and the stainless steel would be. 3D defects distribution of corrode reinforced concrete was also visually identified by X-CT technique. It showed that with sulfate ions added to the concrete including chloride ions, the fractions of micro defects became larger, while the fractions of the macro defects became smaller, which illustrated that the expansion pressure of the corrosion products was reduced and the concrete became more compact under the effect the sulfate ions.

---

**Keywords:** reinforced concrete, accelerated potentiostatic corrosion test, X-CT technique, crack

## 1. INTRODUCTION

Chloride-induced rebar corrosion is one of the major forms of marine environmental attack to reinforced concrete [1]. When corrosion happens on metal surface, the transformation of metallic irons into the oxides would be accompanied with a volume increment up to 4~6 times, which is the root cause for concrete expansion and crack. Oxygen and chloride ions would pass through the crevices easily to accelerate the corrosion process of the steel [2]. Except the temperature and humidity, the corrosion rate is mainly influenced by the concentration of chloride ions and sulfate ions nearby the

rebar [3-4]. The increment of conductivity of concrete and corrosion current density values would improve the corrosion risk of reinforced steel. The results of Bulu Pradhan studies showed that the presence of chloride ions could increase the conductivity of concrete[5]. Abd El Aal et al[6-7] investigated the role of chloride and sulphate ions of rebar corrosion in saturated  $\text{Ca}(\text{OH})_2$  solutions. The sulphate ions were found to be more corrosive than chloride ions. The activation energy, for the propagation of pitting corrosion of steel by  $\text{SO}_4^{2-}$  and  $\text{Cl}^-$  anions were 41.04 and 39.40 KJ/ mol. However, the precise role of sulfate ions in chloride-induced reinforcement corrosion crack of concrete is not very well investigated. The initial cracking time and cracking process of chloride-induced reinforcement corrosion in concrete effected by the couple factors of chloride ions and sulfate ions have not yet been clarified.

Researchers have developed works to evaluate different aspects of corrosion mainly by electrochemical methods and observe the weight-loss of the bars in chloride environment [8]. Considering the natural process of chloride ions entering into concrete and inducing rebar corrosion is too long[9-11], the constant potential accelerated method is often used to get the damage process of reinforced concrete quickly.

Composition and modulus of rebar corrosion product could influence the expansion rate and pressure of the concrete. XRD, SEM, and Nanoindenter are capable to characterize the microstructure [12-13], but can't obtain the multidimensional images of the specimens. X-CT technique could provide a way to obtain 3D and 2D images and defect distribution on materials without any destruction and previous drying treatment, so it is widely applied to study the evolution of microstructure fracture, sulfate attack and carbonation of concrete[14-16].

In this paper, the initial cracking time and cracking process of reinforced concrete mixing with chloride ions, sulfate ions or composite ions were studied by the constant potential accelerated method. The cracking state of concrete cover due to corrosion products volume expanding was visual observed by X-CT technique. The aim of this study is to deepen the recognition of corrosion mechanism of reinforced concrete influenced by the coupled factors of sulfate ions and chloride ions, and to provide a means for nondestructive and visual observation of the corrosion process of reinforced concrete. This work is significant for corrosion control of rebar in the environment of saline soil and coastal area.

## 2. EXPERIMENTATION

### 2.1. Materials and specimen preparation

A Chinese standard P.O.42.5 Ordinary Portland cement, with a compressive strength of 51.4 MPa at an age of 28 days was used. The chemical composition of cement is shown in Table 1. Coarse aggregate was crushed granite with maximum size of 25mm, and river sand with fineness modulus of 2.6 was used as fine aggregate. A naphthalene-type superplasticizer was used and its dosage was adjusted to keep the slump of fresh concrete in the range of 140 and 180 mm.

**Table 1.** Chemical composition of cement

Constituent (wt%)	SiO <sub>2</sub>	Al <sub>2</sub> O <sub>3</sub>	Fe <sub>2</sub> O <sub>3</sub>	CaO	MgO	TiO <sub>2</sub>	Na <sub>2</sub> O	K <sub>2</sub> O	SO <sub>3</sub>	Cl <sup>-</sup>
Cement	20.07	5.09	2.93	61.71	1.58	0.34	0.70	0.36	1.99	0.00

The concrete mixtures were prepared with an effective water-to-cement ratio(w/c) of 0.34 and total cement content of 450kg/m<sup>3</sup>. The mixture proportions and the corresponding compressive strengths of the concretes are given in Table 2.

**Table 2.** Mix proportion and compressive strength of concretes (kg/m<sup>3</sup>)

No	kg·m <sup>-3</sup>				Compressive strength(MPa)	
	Cement	Sand	Aggregate	Water	7d	28d
L50	450	711	1067	155	36.05	53.92

Reinforced concrete specimens were prepared as a square section (100×100mm×400mm). The longitudinal reinforcements were made of two bars (12mm diameter deformed carbon steel bars at the top with an effective cover of 30 mm, and 8mm diameter stainless steel bar at the bottom with an effective cover of 20mm). The steel bars were cleaned and coated with cement paste followed by an epoxy coating at the concrete-air interface. The surface of deformed carbon steel bar was polished by No.200 sand paper. The steel bars were degreased by acetone just prior to be placed in the mold. Reinforced concrete samples were cast and placed at room temperature in the mould, which was removed after 48h. Finally, all specimens were cured in a condition of 20°C±3 °C and 95% relative humidity for 26 days.

2.2 Accelerated corrosion program

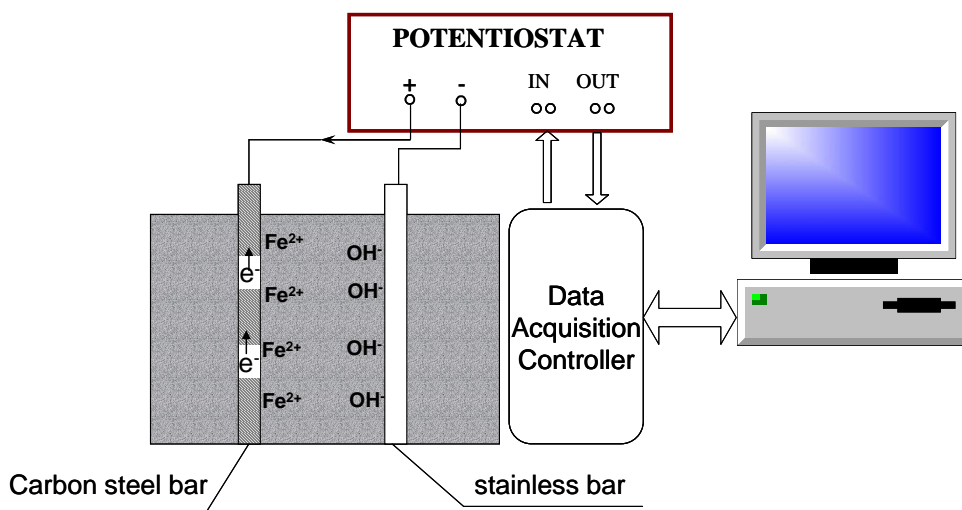


**Figure 1.** Potentiostatic accelerated corrosion of reinforced concrete

As concrete molding, the mixing water, including tap water, chloride solution (0.1%NaCl, 0.25%NaCl, 0.5%NaCl or 1%NaCl), and composite solution (1%NaCl+0.5%Na<sub>2</sub>SO<sub>4</sub>, 1%NaCl+1.5%Na<sub>2</sub>SO<sub>4</sub>) was used.

After concrete were cured for 26 days, their reinforcements were subjected to accelerated corrosion current supplied by potentiostat through deformed carbon steel bar (connect to the positive electrode) and stainless steel bar (connect to the negative electrode). And the electric potential was kept constant as 30V. The current was determined every 2 hours. A diagram of the test can be seen in Fig.1.

### 2.3 Crack width test

The surface of the reinforced concrete specimens was observed daily. The cracks width was completed with a crack test instrument (precision of 0.01mm).

### 2.4 X-CT measurement

X-CT is a three-dimensional imaging technique by using a series of radiographic images to reconstruct a map of X-ray absorption. A sensor was connected to pick up the resulting intensity of recognized unidirectional (x-axis) X-ray beam transformed the materials. According to Beer-lambert's law, for each angle of projection  $\theta$ , the resulting intensity  $I(y, z, \theta)$  on each pixel of the detector (coordinates  $y, z$ ) is given by:

$$I(y, z, \theta) = I_0 \cdot \exp(-\int \mu(x, y, z, \theta) dx) \quad (1)$$

Where  $I_0$  is the intensity of the beam before the sample and  $\mu(x, y, z, \theta)$  stands for a great number of angles  $\theta$ , namely the Radon transform of the attenuation coefficient of the sample. The projection-slice theorem ensures that, for a sufficient specimen sampling, the 3D map of  $\mu$  can be reconstructed. The attenuation coefficient mainly depends on the density and the chemical composition of the materials.

In this work, reinforced concrete samples were examined visually with X-CT system (YXLON, Civil engineering material key lab in Southeast University). The voltage and current of the X-ray tube were 225 kV and 0.65 mA, respectively. The detector type was flat panel Y.XRD1620, and the numbers of detector elements were 1024. The number of projections were 1080. The 2D pixel size was 0.14 mm  $\times$  0.14 mm, pixel numbers were 1024  $\times$  1024. The 3D voxel size was 0.14 mm  $\times$  0.14 mm  $\times$  0.14mm. The object rotation angles are 360 degree.

After the accelerated corrosion test was completed, the cracked samples were filled with epoxy by vacuum method and cured for 3 days. Then the specimens were cut to the size of 100mm $\times$ 100mm $\times$ (20-30) mm for X-CT test.

2.5 surface characterization

The surface morphologies of the specimens were observed by scanning electron microscopy (SEM, KYKY-2800B).

3. RESULTS AND DISCUSSION

3.1 Electric current

Concrete mixed with chloride solutions and composite solutions were polarized by a constant voltage of 30V, and the current change with time is shown in Fig. 2. The electric current decreased fast at the early stage while slowed down as the concrete cracked. Additionally, the electric current intensity increased with the concentration of chloride solution while decreased with the addition of sulfate ions.

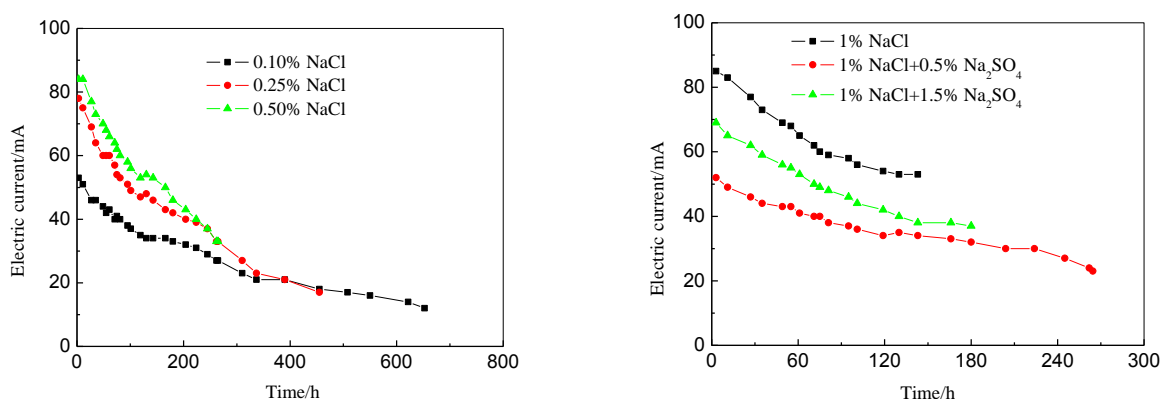


Figure 2. Current evolution of reinforced concrete subjected to potentiostatic accelerated corrosion

Considering the voltage between deformed steel bar and stainless steel bar was 30V, the electric resistance was calculated. The evolution of resistance ratio(R(t)/R(0)) under the potentiostatic accelerated corrosion were obtained, as shown in Fig 3. The relationship between R(t)/R(0) and corrosion age could be regressed by the exponential function as follows:

$$R(t) / R(0) = \exp(a \times t) \quad (2)$$

Where R(t) is the electric resistance of reinforced concrete at ‘t’ time, R(0) is the electric resistance of reinforced concrete at the initial time, t is the corrosion time, and ‘a’ is regression coefficient.

From Fig.3 it can be seen that the electric resistance between deformed carbon steel bar and stainless steel bar increased with the aggravation of corrosion process. There were two reasons for this, the first was that the water transportation from inner to the outer along the carbon steel bar reduced the concrete humidity, the second was that the rust layer on the surface of steel bar fulfilled the concrete matrix, which in turn increase the electric resistance.

As shown in Fig.3, the electric current intensity increased with the concentration of chloride solution. The sulfate ions could improve the electrical resistivity of concrete with low concentration, while would reduce it as the concentration reaching to a high value. The electric resistivity of concrete was influenced by free chloride ion content and compactness of concrete.

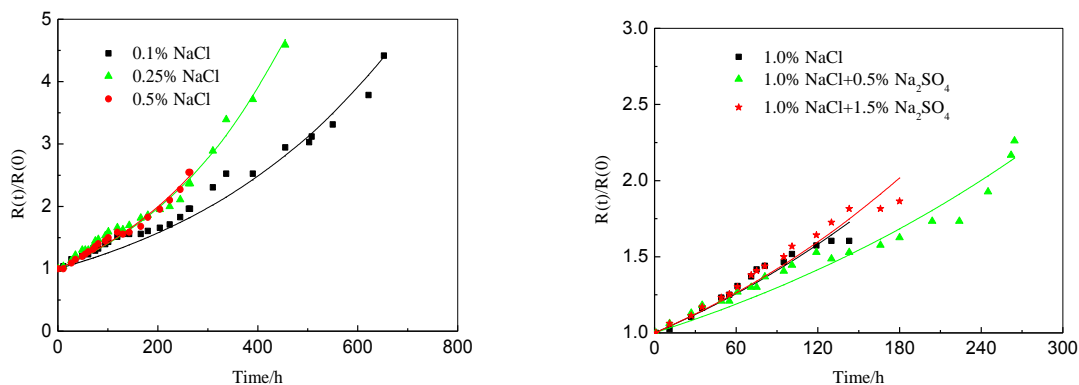


**Figure 3.** Evolution of  $R(t)/R(0)$  of reinforced concrete under potentiostatic accelerated corrosion

According to the exponential function, the coefficient ‘ $a$ ’ was regressed and shown in Table. 3. The value of coefficient ‘ $a$ ’ increases with increasing the concentration of chloride ions. Nevertheless, as 0.5%  $Na_2SO_4$  was added to 1% NaCl solution, ‘ $a$ ’ value declined, while the concentration of  $Na_2SO_4$  increased to 1.5%, ‘ $a$ ’ value increased, which is similar to that of 1% NaCl solution.

**Table 3.** Value of coefficient ‘ $a$ ’ for reinforced concrete mixing with different corrosion solution

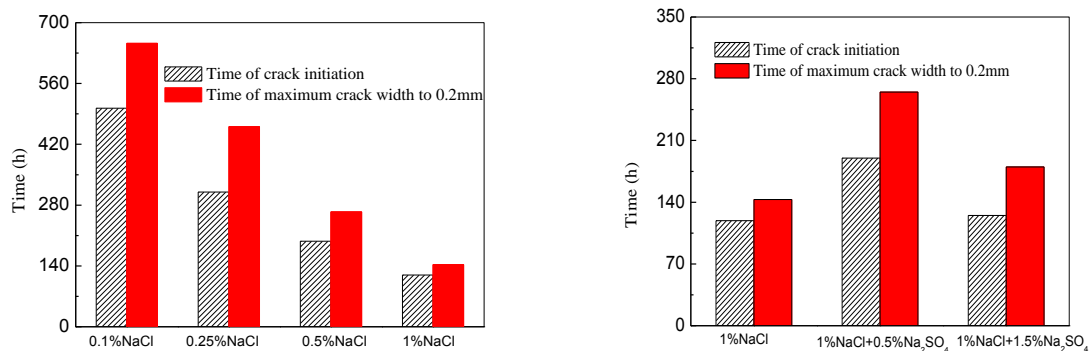
mixing solution	0.1%NaCl	0.25%NaCl	0.5%NaCl	1%NaCl	1%NaCl+0.5% $Na_2SO_4$	1%NaCl+1.5% $Na_2SO_4$
Coefficient $a \times 10^{-3}$	2.27	3.39	3.45	3.82	2.89	3.90

### 3.2 Cracking process

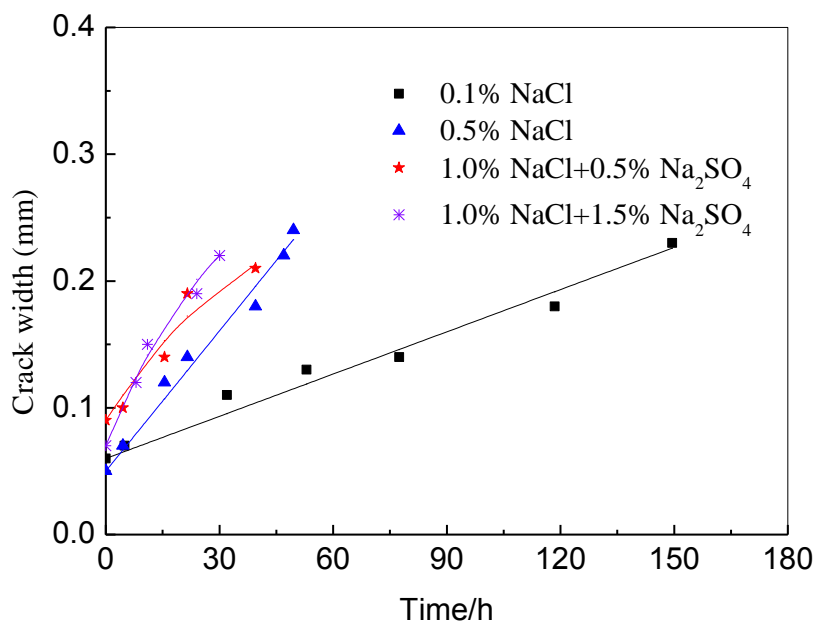
The time of crack initiation and maximum crack width reaching to 0.2mm was shown in Fig. 4. It was clearly that the initial cracking time reduced with the increment of chloride concentration, which indicated that the crack expanding process was accelerated by the chloride ions. As the sulfate ions adding to the mixing water, the time of crack initiation and crack expansion was prolonged. In different solutions, the changing curves of crack width with time were shown in Fig.5.

Fig.5 indicated that the crack propagation of concrete in single chloride environment is linearly increases with time. Since the corrosion products of reinforced bar increases linearly with chloride ions content and time, the elastic modulus of corrosion products and tensile strength influenced by chloride

ions content and corrosion time should be neglected. Therefore, the expansion pressure of corrosion products increased with corrosion, and resulted to the linearly crack of reinforced concrete. However, as the reinforced bar in reinforced concrete was surrounded by sulfate ions plus chloride ions, the cracking process resulted from steel bar corrosion was accelerated at the early stage. The results may be attributed to the increment of elastic modulus of concrete and the looseness of the corrosion products to disperse the swelling stress.



**Figure 4.** Time of crack initiation and maximum crack width to 0.2mm of reinforced concrete with different solutions



**Figure 5.** Crack propagating of reinforced concrete with corrosion time

Based on the experimental results, the cracking process of reinforced concrete could be regressed by the linear functions and quadratic functions, which was shown in Table 4. Where, x is time, y is crack width, R is correlation coefficient.

**Table 4.** Functional regression of cracking process of reinforced concrete with different mixing water

Mixing water	Functions	Correlation coefficient R <sup>2</sup>
0.1% NaCl	$y=0.06+0.00111x$	0.975
	$y=0.06+0.00121x-8.413*10^{-7} * x^2$	0.976
0.5% NaCl	$y=0.05+0.00369x$	0.981
	$y=0.05+0.00422x-1.332*10^{-5} * x^2$	0.983
1.0% NaCl+0.5% Na <sub>2</sub> SO <sub>4</sub>	$y=0.09+0.00338x$	0.91
	$y=0.09+0.0047x-0.00004 * x^2$	0.95
1.0% NaCl+1.5% Na <sub>2</sub> SO <sub>4</sub>	$y=0.07+0.00521x$	0.95
	$y=0.07+0.0074x-0.00008 * x^2$	0.98

Apparently, as the reinforced bar in concrete was located in single chloride ions environment, the crack propagation could be expressed by linear function, which meant that the cracking process resulted from steel bar corrosion was uniform. However, as the reinforced bar in concrete was surrounded by composite environment including chloride ions and sulfate ions, the correlation coefficient of quadratic function was higher than that of the linear function. In this case, the cracking process resulted from steel bar corrosion was accelerated at the early stage, but as the crack width reaching to a certain value, it became stable.

As 0.5%Na<sub>2</sub>SO<sub>4</sub> adding to the chloride salt water, the time of crack initiation and crack expansion was prolonged. Further, when the concentration of Na<sub>2</sub>SO<sub>4</sub> in chloride salt water reached to 1.5%, the time of crack initiation and crack expansion was decreased. Due to NaCl and Na<sub>2</sub>SO<sub>4</sub> mixed in water as concrete was casted; the chloride ions concentration nearby the steel bar is more than the critical chloride ions content[6-7], the sulfate ions and chloride ions concentration have little effect on the time to initiation of reinforcement corrosion. Therefore, the time of crack initiation and crack expansion would be effected by tensile strength of concrete and expansion press of corrosion products on the surface of steel bar. Furthermore, the expansion press was linearity correlation to the corrosion products content and its Elastic modulus. More chloride ions concentration nearby the steel bar, more increment of corrosion products was grown in the interface zone of concrete and steel bar and led to the higher expansion pressure. And finally, the time of crack initiation and crack expansion was reduced.

Due to the conjoint presence of chloride and sulfate ions, free chloride ions concentration increased, which promoted the corrosion products growth. The increase in concentration of free chloride ions was ascribed to the total chloride ions and the simultaneous reaction of C<sub>3</sub>A with both chloride and sulfate ions, as a result, the proportion of chloride ions bounded was less than that of chlorides salts. Therefore, the free chloride ions content would be increased when sulfate ions were presented. Additionally, the sulfate ions would react with the cementitious compounds, promoting the formation and growth of ettringite and gypsum, resulting in promotion of the pores pressure, and then leading to microcracking and decrement of concrete compactness. However, a small amount of crystals

could fill the pore and some the concrete defects, and then increased its compactness as the concrete with low concentration of sulfate ions at the early corrosion period.

### 3.3 Analysis by X-CT technique

The 2D images of the concrete specimens mixing with 1%NaCl and with 1%NaCl+0.5%Na<sub>2</sub>SO<sub>4</sub> were shown in Fig.6 and Fig.7. The aggregate, reinforced bar, and cracks distribution in concrete were able to be evidently distinguished according to the gray scale of images.

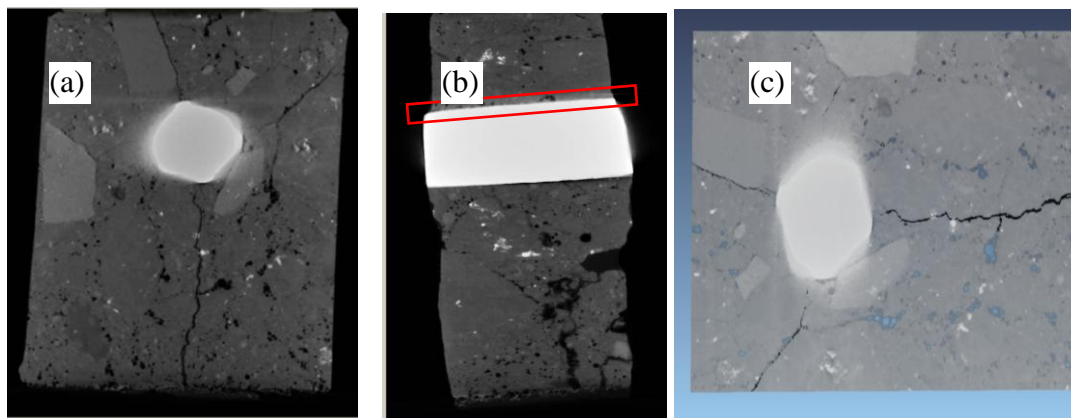


**Figure 6.** 2D image of reinforced concrete specimens mixing with 1%NaCl (a) front view (b) vertical view (c) panorama

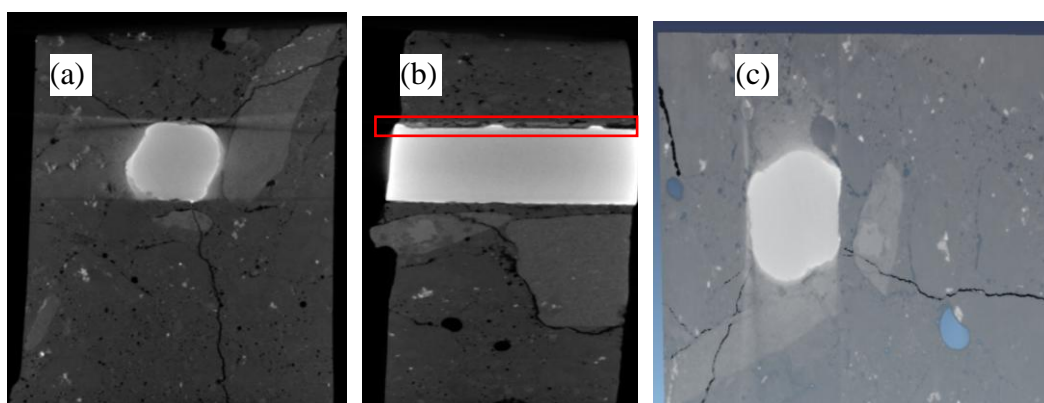
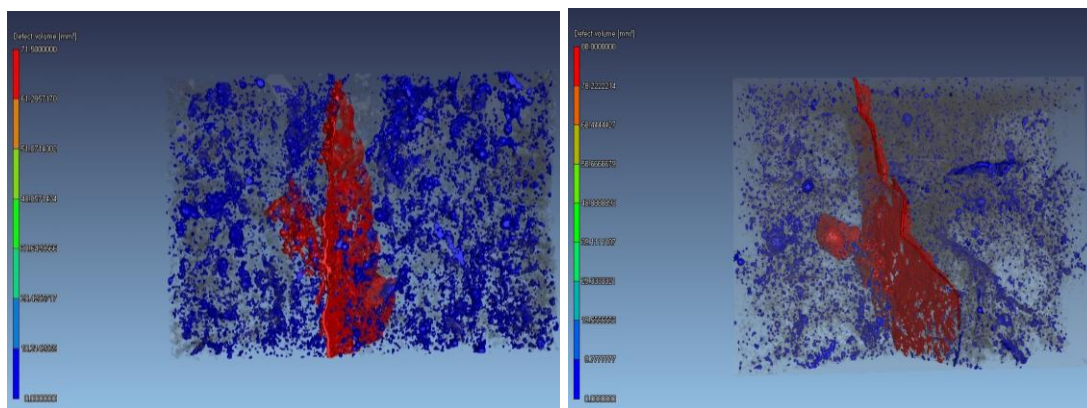


**Figure 7.** 2D image of reinforced concrete specimens mixing with 1%NaCl+0.5%Na<sub>2</sub>SO<sub>4</sub> (a) front view (b) vertical view (c) panorama

The chloride-induced corrosive crack expanded from the center of reinforced bar to the matrix, some of them even penetrated to the aggregate. The crack width on the concrete surface was larger than that nearby the reinforced bar. The corrosion products layer, marked in the red box of Fig.6(b) and Fig.7(b), mainly located on the top surface of reinforced bar with about 1.0mm thickness and 5.10g/m<sup>3</sup> density. The density value was between the concrete and steel, which can be proved by the gray scale.

Fig.8 shows 3D defects distribution of reinforced concretes. In order to obviously distinguish the defects volume, the multicolor from blue to red was used to represent the defects volume from small to large. It can be seen that the large scale defects were mainly located nearby the reinforced concrete. The cracks were connected to each other and expanded from the reinforced bar to the surface of the concrete.



(a) mixing with 1%NaCl

(b) mixing with 1%NaCl+0.5%Na<sub>2</sub>SO<sub>4</sub>

**Figure 8.** 3D stereoscopic images and defects distribution of reinforced concrete

For quantitative analyzing the effect of rebar corrosion on concrete damage under the environment including single chlorine salt and compound salt, the defect volume amount and distribution of reinforced concretes were calculated, as shown in Fig.9(a) and (b). It was clearly that the micro-defects ( $\leq 0.01\text{mm}^3$ ) volume fractions of concrete mixing with composite solution was approximately 1.5 times more relative to that only with chloride ions, which indicated the existence of sulfate ions could refine the concrete materials at the early stage.

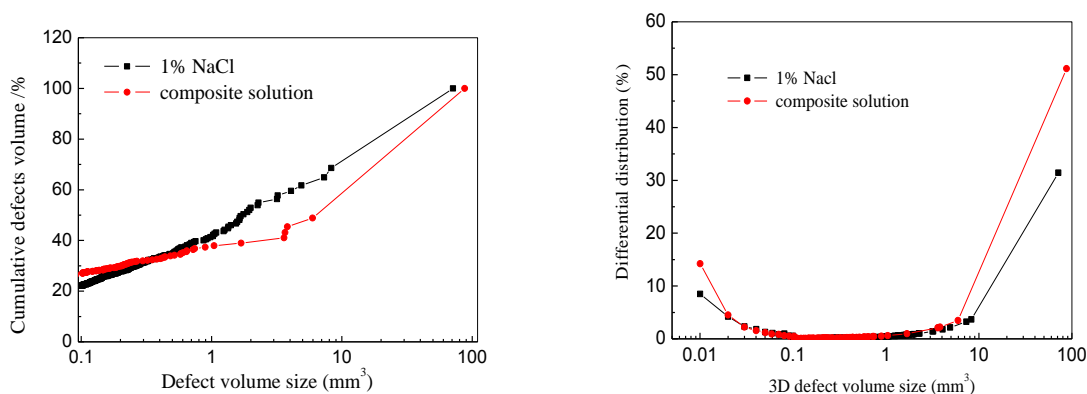


**Figure 9.** 3D defect volume distribution of reinforced concretes with 1% NaCl and composite solution

The meso-defects ( $0.01\text{ mm}^3 \leq \text{meso-defect} \leq 1\text{ mm}^3$ ) volume fractions of the two types of concrete roughly had the same size. However, the middle size cracks ( $1\text{ mm}^3 \leq \text{defects volume} \leq 5\text{ mm}^3$ ) volume fractions of concrete mixing with chloride solution was approximately 2.4 times than that of

mixed with composite solution, which indicated that the existence of sulfate ions in combination solution reduced the expansion pressure of the corrosion products. Therefore, the time to reach the maximum crack width induced by chloride ions was prolonged by sulfate ions.

### 3.4 SEM analysis

SEM images of the corrosion samples taken from the interface of corroded reinforced bar and concrete was shown in Fig.10. A close observation revealed that the corrosion products were compact and massive as concrete mixing with chloride solution, while became thin and granulate as concrete mixing with composite solution, which also proved that the existence of sulfate ions could lighten the expansion pressure caused by corrosion products, which was in agreement with the results of previous research[18].

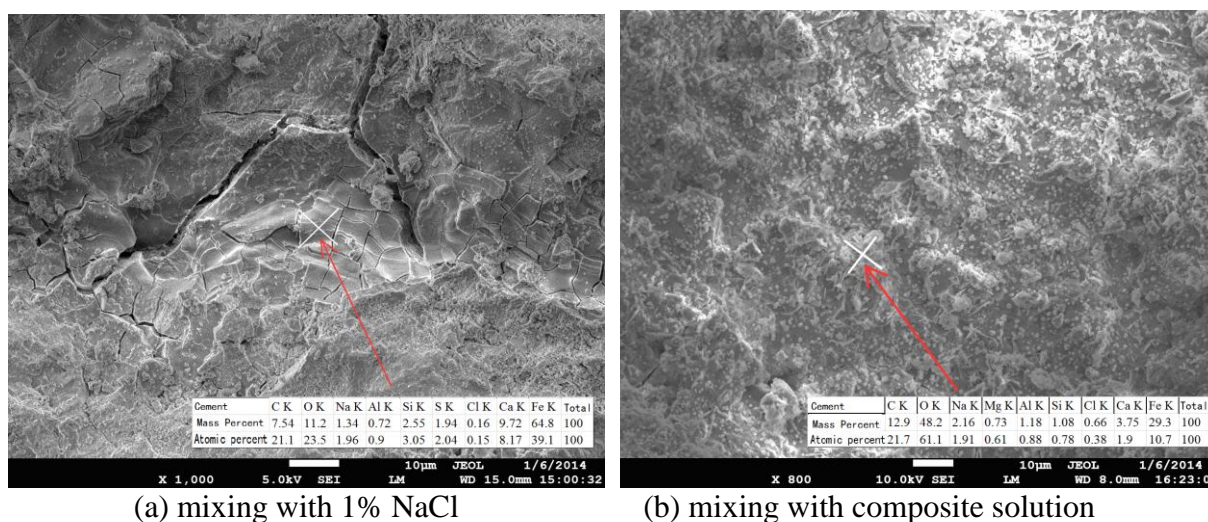


**Figure 10.** SEM image of interface of corroded reinforced bar and concrete

## 4. CONCLUSIONS

As reinforced concrete mixed with chloride solution or composite solution subjects to potentiostatic accelerated corrosion, the current decreased linearly with time without crack, but slowed down as crack happened.

The time of initial cracking and maximum crack width reaching to 0.2mm of reinforced concrete decreased with increasing the concentration of chloride ions in mixed water, and the crack propagation of concrete in single chloride environment is linearly increased with time.

As 0.5%Na<sub>2</sub>SO<sub>4</sub> adding to chloride salt water, the time of crack initiation and crack expansion was prolonged. Furthermore, as the concentration of Na<sub>2</sub>SO<sub>4</sub> in chloride salt water increasing to 1.5%, the time of crack initiation and crack expansion decreased. The crack propagation of reinforced concrete in the environment including sulfate ions and chloride ions would be formed quickly at the initial time, and then increased slowly.

X-CT technique is helpful in visual identification of 3D defects distribution of concrete by nondestructive approach and comprehensively investigation on the microstructure evolution of reinforced concrete subjected to chloride-induced corrosion.

#### ACKNOWLEDGMENTS

This work is part of a series project financially supported by the Chinese National Natural Science Foundation (NSF) Grant No. 51178230, No. 51378269, and the Qingdao Science and technological Foundation Grant No.13-1-4-176-jch, No. 13-1-4-115-jch. Except from it, this work is also supported by the Open Fund of Key Laboratory of Marine Environmental Corrosion and Bio-fouling (MCKF201404). The authors gratefully appreciate the financial support provided by the NSF and other Foundations.

#### References

1. X. Shi, N. Xie, K. Fortune, *Constr. Build. Mater.* 30 (2012) 125.
2. R. Raquel, Avela, N.F.Ortega, *Constr. Build. Mater.* 25 (2011) 630.
3. A. Alhozaimy, R. R. Hussain, R. Al-Zaid, *Constr. Build. Mater.* 28 (2012) 670.
4. S. D.Gustavo, S.B. Farina, *Constr. Build. Mater.* 23 (2009) 2746.
5. B. Pradhan, *Constr. Build. Mater.* 72 (2014) 398.
6. E.E. Aal, S. Wanees, A. Diab, S.M.Haleem, *Corros. Sci.* 51 (2009) 1611.
7. S. Haleem, S. Wanees, A. Bahgat, *Corros. Sci.* 75 (2013) 1.
8. M. Moreno, W. Morris, M.G.Alvarez, G.S. Duffó, *Corros. Sci.* 46 (2004) 2681.
9. T. Cheewaket, C. Jaturapitakkul, W. Chalee, *Constr. Build. Mater.* 37 (2012) 693.
10. W. Xue, L. Zhang, Y. Xiong, J. Chen, W. Jin, *Procedia Eng.* 27 (2012) 1635.
11. X.Wang, X.Jin, Y.Tian, *J.Zhejiang Univ.* 47 (2013) 1.
12. R. Veraa, M. Villarroel, A. M. Carvajal, *Mater. Chem.Phys.* 114 (2009) 467.
13. Y. Zhao, H. Dai, W. Jin, *Corros. Sci.* 65 (2012) 163.
14. E. N. Landis, E. N. Nagy, D. T. Keane, *J. Eng. Mech.* 70 (2003) 911.
15. S. R. Stock, N. K. Naik, A. P. Wilkinson, *Cement Concrete Res.* 32 (2002) 1673.
16. J.Han, G.Pan, W.Sun, *J. Chin. Ceramic Soc.* 39 (2011) 75.
17. M. Maes, N. D. Belie, *Cement Concrete Comp.* 53 (2014) 59.
18. R. Vera, M. Villarroel, A.M. Carvajal, E. Vera, C. Ortiz, *Mater. Chem.Phys.* 114 (2009) 467.

© 2015 The Authors. Published by ESG ([www.electrochemsci.org](http://www.electrochemsci.org)). This article is an open access article distributed under the terms and conditions of the Creative Commons Attribution license (<http://creativecommons.org/licenses/by/4.0/>).